Proceedings World Geothermal Congress 2023
Beijing, China, April 17 – 21, 2023

Design of a Compact Flat Heat Exchanger for a Modular Thermoelectric Stack Towards Geothermal Power Generation

Entong Xia[1], Heping Xie[1, 2*], Licheng Sun[1*], Xiting Long[2], Jun Wang[2], Cunbao Li[2], Mingzhong Gao[1, 2], Tianyi Gao[1]

1. State Key Laboratory of Hydraulics and Mountain River Engineering, College of Water Resource & Hydropower, Sichuan University, Chengdu, 610065, China

2. Guangdong Provincial Key Laboratory of Deep Earth Sciences and Geothermal Energy Exploitation and Utilization, Institute of Deep Earth Sciences and Green Energy, College of Civil and Transportation Engineering, Shenzhen University, Shenzhen, 518060, China

Corresponding E-mail: xiehp@scu.edu.cn (Heping Xie), leechengsun@sohu.com (Licheng Sun)

Keywords: Geothermal power generation; Compact heat exchanger; Flow uniformity; Modular design

ABSTRACT

Thermoelectric generators (TEGs) own advantages of no moving parts, scalability, and compatibility with different systems. Using of TEG technology for geothermal power generation has been of interest to many researchers in spite of its low conversion efficiency. As such, compactness of a thermoelectric device is of significance for a large-scale application, otherwise it would be too large to become impracticable. In the current work, a compact heat exchanger was designed for a modular thermoelectric stack on the basis of previous work of our research team with foremost aim at realizing large-scale geothermal power generation using of TEG technology. It realizes a uniform flow distribution among sub-channels for a better temperature uniformity across the contacting surfaces with the TEG modules. More importantly, relatively high compactness of the heat exchanger is not at the expense of increasing the flow resistance. Due to that the tapering inlet and outlet play a key role in regulating the flow distribution among the sub-channels, a CFD analysis is be carried out on the current design with modified inlet and outlet, aiming to find optimized design of the heat exchanger. Hence, a comparison of simulation results obtained under given various geometry of tapering inlet and outlet is analyzed, in order to determine an appropriate geometry to weigh the uniformity against flow resistance. Meanwhile, the flow distribution among sub-channels in the heat exchanger is assessed quantitatively. Finally, a compact heat exchanger is designed and optimized, hopefully it can provide a feasible approach to the design of heat exchangers for a large-scale thermoelectric system.

1. INTRODUCTION

Some traditional technologies for geothermal power generation mainly rely on function of mechanical components, such as dry steam power generation, flash steam power generation, binary cycle power generations (Qiu and Hayden 2012; Gholamian et al. 2018; Zare and Palideh 2018). Those technologies have been developed on a larger scale in recent years, and the global installed capacity reaches 14.1 GW by 2020 according to U.S. EIA (Energy Information Administration). However, geothermal power generation has been far behind wind energy (735GW) and solar energy (716 GW) in both growth rate and installed capacity, due to the disadvantages of high initial investment, long payback time, complex system operation, and low conversion efficiency (Li et al. 2015).

Thermoelectric generators (TEG) can directly convert heat into electric under a condition of temperature difference, which have been widely concerned on aerospace and waste heat utilization since 1960s (Tohidi et al., 2022; Lorenz et al, 2020; Xu et al, 2019), due to its competitive edge of green, safety, long lifespan and noiseless operation (Champier 2017). Li et al. (2015) pointed out that thermoelectricity technology may be a breakthrough solution in the field of geothermal power generation. Besides owning most of the advantages of solar PV, it is more stable and scalable than solar PV (Li et al, 2019). Afterwards, Xie et al. (2018) systematically proposed the principle and technological conception of middle-low temperature geothermal power generation based on large-scale single crystal thermovoltaic materials, and comprehensively expounded the key problems and major challenges in implementation of TEG for geothermal power generation. At the current stage, a large-scale application of the technology based on thermoelectric converter has not been carried out on the aspect of geothermal power generation, and it is still in the stage of theoretical research and testing in the laboratory (Catalan et al, 2019; Li et al, 2020; Alegria et al, 2022).

This limitation is caused by the low conversion efficiency of TEG system due to the relatively small value of the figure of merit ($ZT \leq 1$) of currently commercial thermoelectric materials (Zwab et al, 2022). In addition to the improvement in the intrinsic ZT value of thermoelectric materials, optimizing the design of TEGs system is also an alternative solution towards scale utilization (Bell 2008). The heat exchanger is an important TEG component that determines the heat transfer rate from the heat resource to the TEG module as well as the temperature difference of cold side and hot side of TEG. Choice and optimization of heat exchangers is a crucial part of design process for thermoelectric power generators. As such, compactness of a thermoelectric device is of significance for a large-scale application, otherwise it would be too large to become impracticable.

In the current work, a compact heat exchanger was designed for a modular thermoelectric stack on the basis of previous work of our research team with foremost aim at realizing large-scale geothermal power generation using of TEG technology. Due to the significant influence of manifold structure of the heat exchanger on the flow uniformity, a CFD analysis is carried out on given several designs. Based on a comparison of the simulation results, appropriate geometry parameters of current heat exchanger are specified to weigh the flow distribution uniformity against flow resistance.

2 DESIGN OF A COMPACT FLAT HEAT EXCHANGER

2.1 Concept of a Modular Thermoelectric Stack

To achieve a modular assembly of TEGs that promotes its large-scale utilization for heat harvesting, a plate-shape heat exchanger design was proposed by our research team (Yang et al., 2021). The heat exchanger is designed with multiple straight flow sub-channels combined with tapering inlet and outlet, by which a more uniform flow distribution and low flow resistance was realized. With this heat exchanger a modular TEG is proposed, as shown in Figure. 1. More detailed description for this modular design can be seen in the reference (Yang et al., 2021).

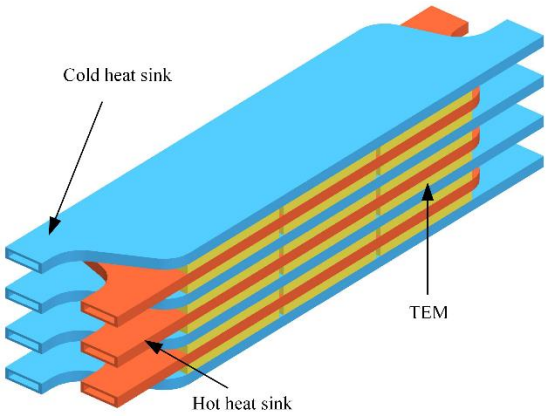

Figure 1: A modular thermoelectric stack towards geothermal power generation

2.2 Geometry of Flat Heat Exchanger with Tapering Inlet and Outlet

Geometry of the flat heat exchanger for the thermoelectric conversion system is shown in Figure 2. Accordingly, its baseline dimensions are given in Table 1. For a further detailed description of the tapering structure, the angle between the side wall and the vertical direction is defined as the inlet wall angle (α_{in}) or the outlet wall angle (α_{out}), and the angle between the line formed at the end of each rib and the vertical direction is defined as the inlet rib angle (β_{in}) or the outlet rib angle (β_{out}). Two round corners in the inlet and outlet have the same radius (R_1 and R_2) respectively. In order to investigate the influence of inlet and outlet with tapering structure on the flow distribution among the sub-channels, various geometry of tapering inlet and outlet are given, aiming to find an optimized design of the heat exchanger that weigh the flow uniformity against flow resistance.

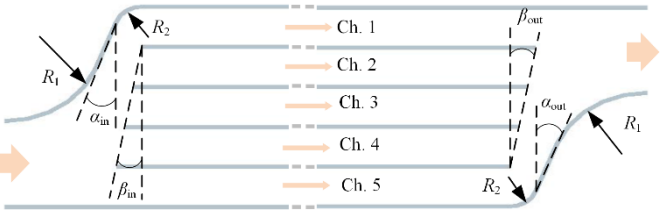

Figure 2: Structure of the tapering inlet and outlet of heat exchange.

Table 1: Baseline dimensions of compact heat exchanger.

Number	Parameter	Value	Unit
1	Length of channel	258	mm
2	Width of sub-channel	8.8	mm
3	High of channel	1.25	mm
4	Number of sub-channels	5	-
5	Width of rib	1	mm

2.3 Solution method

A turbulent flow may occur locally due to the discontinuity of tapering structure even at small hydraulic diameters and low Reynolds number. CFD software of ANSYS FLUNENT is employed as the platform to carried out numerical work. For the current work, the COUPLED algorithm is applied to solve the governing differential equations to obtain the velocity, pressure within the heat exchanger. A standard scheme of the second order upwind is adopted for discretization of the momentum equations. A constant velocity inlet (v_0=1.51 m/s) are set for the boundary conditions. The solutions are considered to be converged when the residual values are less than 10^{-6}.

2.4 Grid Independence Verification

The accuracy of numerical simulation results is related to the number of grids. The grid independence verification is necessary to select an appropriate number of grids that ensures that further increase of the grid number has negligible impact on the calculation results. In this paper, the distribution ratio in each sub-channel and pressure drop between inlet and outlet of heat exchanger is

considered as two key indicators to determine the number of grids. The results of distribution ratio in each sub-channel and pressure drop versus number of grids are shown in Figure 3. As seen from Figure 3, when the number of grids increases from 0.8 to 1.6 million, the maximum change rate of flow distribution ratio of each sub-channel is no more than 0.02%, and the change rate of pressure drop is only 0.03%. Therefore, the number of grids is selected as about 0.8 million for further calculation.

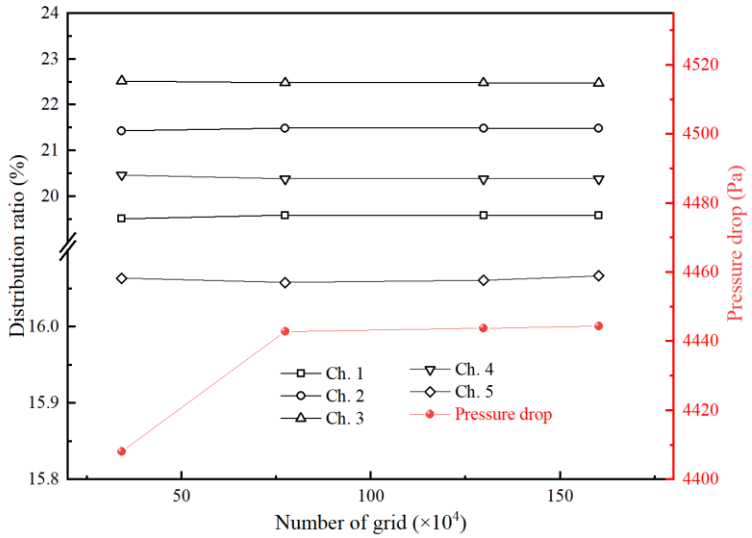

Figure 3 Distribution ratio and pressure drop versus grid number ($\alpha_{in}=\alpha_{out}=20°$, $\beta_{in}=\beta_{out}=0°$, $R_1=20°$, $R_2=5°$)

2.5 Evaluation of Flow Distribution Characteristics

In order to clearly describe the liquid distribution among the sub-channels, distribution ratio (DR) is introduced and defined as the ratio of the mass flow rate in each sub-channel to the total mass flow rate

$$DR = \frac{m_i}{m_t} \tag{1}$$

Standard deviation (SD) is used to represent the total flow maldistribution among the sub-channels, given by

$$SD = \sqrt{\frac{1}{n}\sum_{i}^{n}\left(\frac{m_i}{m_a}-1\right)^2} \tag{2}$$

A more uniform of flow distribution is achieved as SD is close to 0.

where m_i represents the mass flow rate of the ith sub-channel; m_t represents the total mass flow rate inside heat exchange; m_a represents the average mass flow rate inside heat exchange; n is the number of sub-channels.

3 RESULTS AND DISCUSSION

3.1 Analysis of general flow features

It is necessary to provide a description of the general flow features inside the heat exchanger with tapering structure. A comparison of the flow inside configuration A (without smooth round corner) and configuration B (with smooth round corner) are carried out and the results of velocity contours and static pressure are exhibited in Figure 4. As seen from the velocity contours (Figure 4a), there is same flow characteristics between configuration A and configuration B. Flow separation occurs at the entrance of each sub-channel. The strength and size of the reversed flow region rely significantly on the location of the individual sub-channels. The values and distribution of velocity of each sub-channel vary from one sub-channel to another. The velocity contours indicate high velocity values at the middle sub-channel (Ch. 2-3) of heat exchanger, which reflects the result of the flow separation features among sub-channels. Therefore, it is expected that a flow maldistribution is caused by this flow feature.

Accordingly, the pressure contours (Figure 4b) indicate the non-uniformity of pressure distribution insider heat exchanger. It is obvious that the high-pressure values are presented at the upstream of the inlet header, and the pressure values of the configuration B is significantly reduced than that of configuration A. Calculation demonstrates that the pressure difference between inlet and outlet of heat exchanger for configuration A reaches 7693 Pa, while only 4442 Pa for configuration B. It is reduced by 42.2%, which is because that the recirculated flow region around the corner is eliminated by using smooth round corner rather than sharp corner.

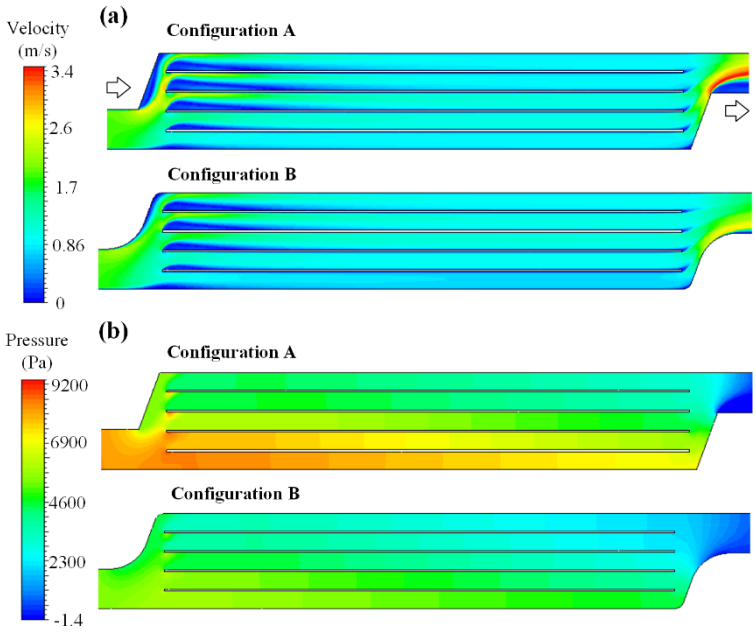

Figure 4: General flow features for configuration A (without smooth round corner) and configuration B (with smooth round corner): (a) velocity magnitude at midplane; (b) static pressure distribution at midplane.

3.2 Influence of Wall Angle (α)

Four values of 15°, 20°, 25° and 30° for α are specified to investigate the influence of α on the flow distribution inside heat exchanger. The variation tendency of mass flow rate of each sub-channel is shown in the Figure 5 for different value of α, accordingly, the pressure drop through the heat exchanger and flow maldistribution are also depicted in Figure 6. Based on its definition in Eq. (2), a smaller value of standard deviation (SD) for flow distribution reflects the lower level of non-uniformity.

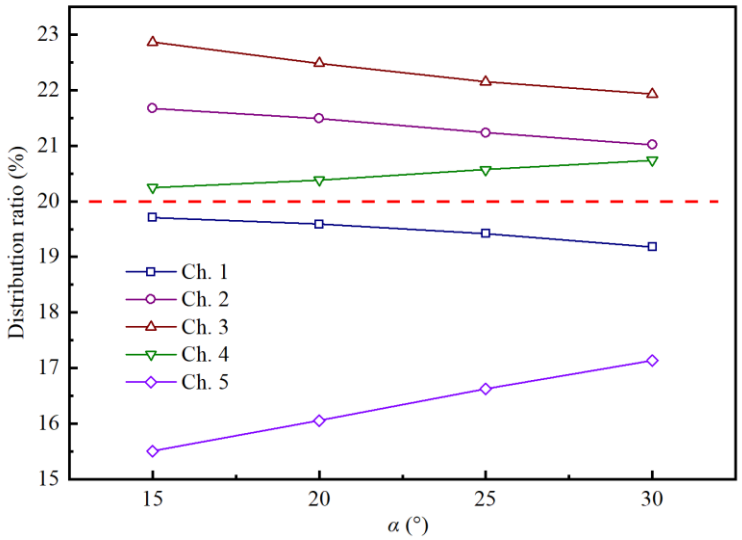

Figure 5: The variation of the mass flow rate of each sub-channel under different α ($\alpha=\alpha_{in}=\alpha_{out}$, $\beta_{out}=\beta_{in}=0°$, $R_1=20°$, $R_2=5°$).

When α is equal to 15°, more fluid is distributed to the sub-channels away from the inlet (Ch. 1-4), and the sub-channel near the inlet (Ch. 5) receives the least fluid. In this case, the maximum value of the mass flow rate is about one and a half times the minimum value among sub-channels. The non-uniformity of fluid distribution inside heat exchange is the most serious, and the flow maldistribution reaches 12.5%. Increasing the value of α has a significant increment on the mass flow rate of Ch. 5, while only brings about to change slightly for Ch. 1-4.

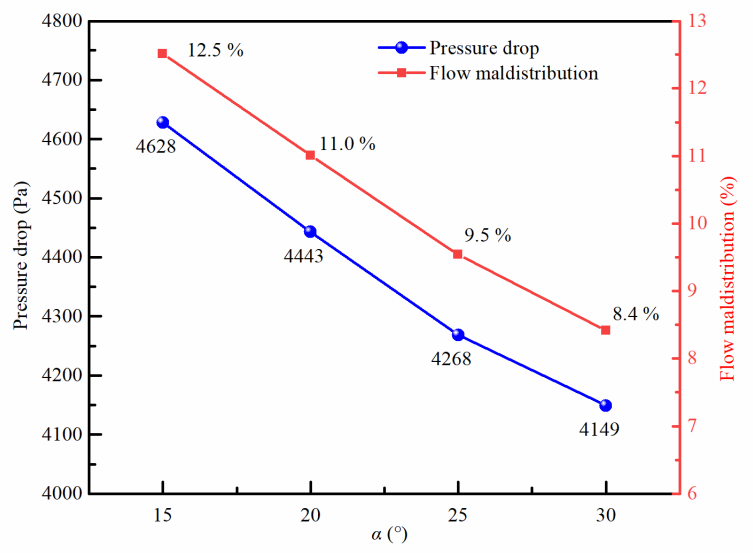

Figure 6: The influence of α on the flow distribution and pressure drop ($\alpha=\alpha_{in}=\alpha_{out}$, $\beta_{out}=\beta_{in}=0°$, $R_1=20°$, $R_2=5°$).

As presented in Figure 6, both of the flow maldistribution and the pressure drop are reduced when α is increased from 15° to 30°. It is noticed that the decline of flow maldistribution becomes slower when α varies from 25° to 30° than that when α varies from 20° to 25°. In addition, a larger α brings about a reduction of the installation space for other components in TEGs system, and it is to the disadvantage of the compact design of TEGs system. Consequently, it is recommended to 25° as the wall angle.

3.3 Influence of Rib Angle (β)

Considering inlet rib angle (β_{in}) is equal to outlet rib angle (β_{out}), both are changed identically. The influence of rib angle (β) on the distribution of mass flow rate among each sub-channel is shown in Figure 7 for different values of β. The figure indicates that increasing β resulting in a rapid linear increase of the mass flow rate of Ch. 1, and a sharp decrease of the mass flow rate of Ch. 4. It may be an ineffective design for an outlet rib angle equal to an inlet rib angle.

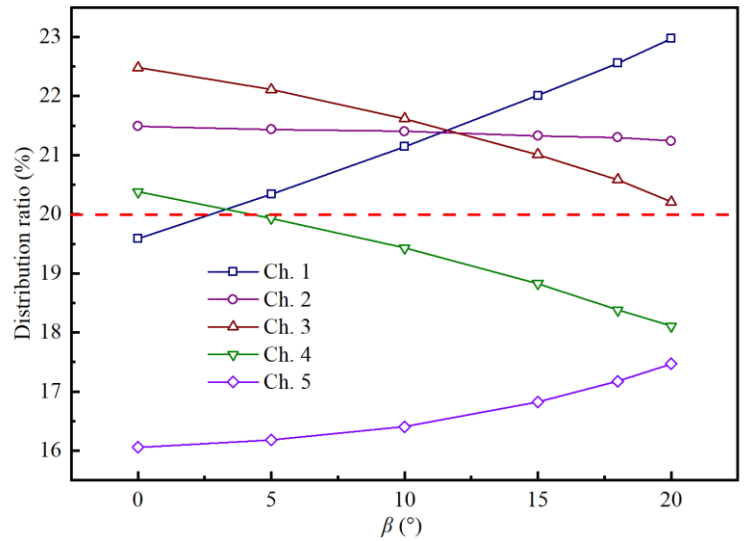

Figure 7: The variation of the mass flow rate in each sub-channel under different β ($\alpha_{in}=\alpha_{out}=20°$, $R_1=20°$, $R_2=5°$).

Figure 8 presents a quantitative result for total flow maldistribution and pressure drop between inlet and outlet under different β. As shown in Figure 8, the flow maldistribution decreases to a minimum value at β=15° from a maximum value at β=0°, then increases to a higher value at β=20°. Correspondingly, the variation of pressure drop is rapid and the pressure drop is increased by 26.4 % from β=0° to β=15°. Therefore, it is expected that the relatively high uniformity of flow distribution insider the heat exchanger is not at the expense of increasing the flow resistance.

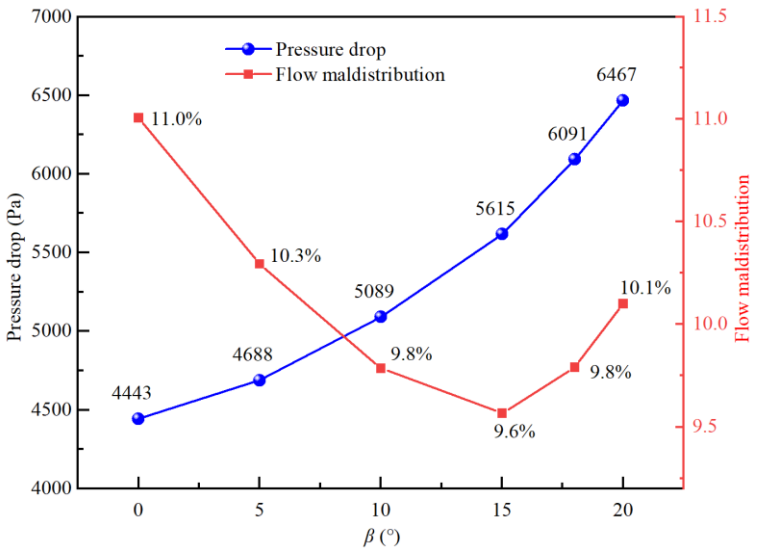

Figure 8: The influence of β on the flow distribution and pressure drop ($\alpha_{in}=\alpha_{out}$ =20°, R_1=20°, R_2=5°).

3.4 Influence of Inlet Rib Angle (β_{in})

The result of the influence of inlet rib angle (β_{in}) on the distribution ration of the mass flow rates in each sub-channel is shown in Figure 9. Increasing of the β_{in} has significant influence on the distribution of fluid among sub-channel. As shown in Figure 9, the mass flow rate of Ch. 4-5 near the inlet increases nonlinearly when β_{in} increases from 0° to 22°, while that of Ch. 1-3 away from the inlet decreases nonlinearly. Especially, the distribution ratio of Ch.5 can reach 20%, since the separation region at the entrance of Ch.5 is smaller due to an increase of the length of rib near the inlet.

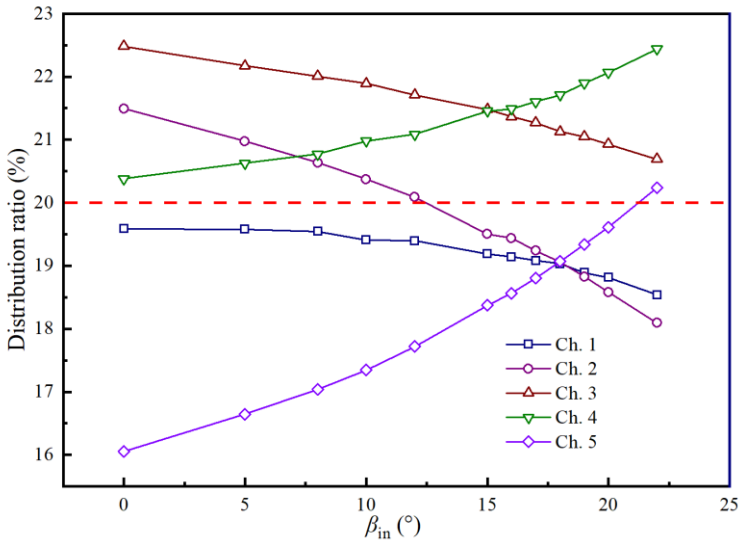

Figure 9: The variation of the **mass flow rate in each sub-channel under different β_{in} ($\alpha_{in}=\alpha_{out}$ =20°, β_{out}=0°, R_1=20°, R_2=5°).**

Figure 10 shows the influence of β_{in} on the flow distribution and pressure drop. The tendencies of both of flow maldistribution and pressure drop at α=20° are consistent with that at α=25°. Compared with the results of Figure 8, the pressure drop is further reduced and the uniformity of fluid distribution is significantly improved due to β_{out}=0°. It is worth noting that the value of flow maldistribution is smallest at this case of β_{in}=18°, even if the pressure drop increases rapidly when β_{in} increases from 0° to 25°. In addition, as can be seen in Figure 10, the uniformity of the flow distribution in heat exchange is optimal in this case of both α=25° and β_{in}=18°, and total flow maldistribution is only 4.6% with a pressure drop of 4826 Pa.

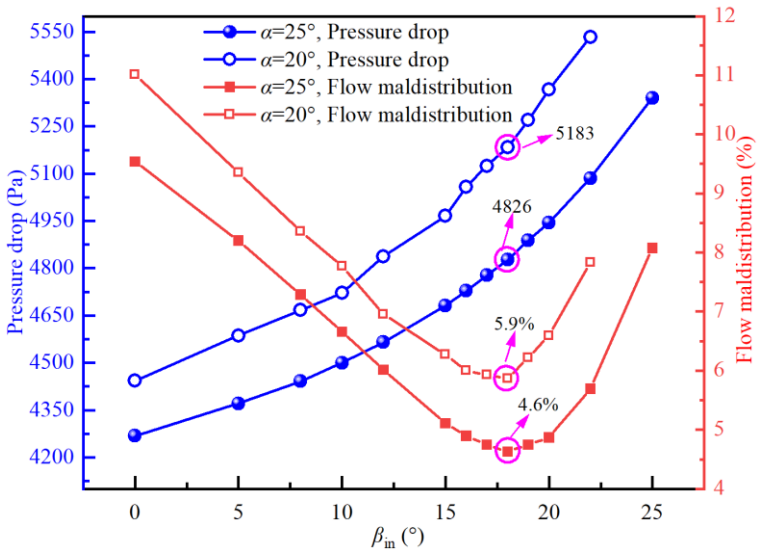

Figure 10: The influence of β_{in} on the flow distribution and pressure drop (β_{out}=0°, R_1=20°, R_2=5°).

4 CONCLUSION

In the current work, a CFD analysis will be carried out on a further modification for tapering inlet and outlet of a compact heat exchanger on the basis of previous work of our research team. Several structures of tapering inlet and outlet for current heat exchanger are compared with respect to the velocity distribution in flow channels and pressure drop between inlet and outlet. A comparison of simulation results revealed that the synergy of wall angle and rib angle has a significant influence on the uniformity of flow distribution and pressure drop. The uniformity of the flow distribution in heat exchange is optimal in this case of α=25°, β_{in}=18°and β_{out}=0°, and total flow maldistribution is only 4.6% with a moderate pressure drop of 4826 Pa.

REFERENCES

Alegria, P. Catalan, L.: Araiz M.: Experimental development of a novel thermoelectric generator without moving parts to harness shallow hot dry rock fields, *Applied Thermal Engineering*, **200**, (2022), 117619.

Bell, L.E.: Cooling, heating, generating power, and recovering waste heat with thermoelectric systems, *Science*, **321**, (2008), 1457–1461.

Champier, D.: Thermoelectric generators: A review of applications, *Energy Conversion and Management*, **140**, (2017), 167–181.

Catalan, L., Aranguren, P., Araiz, M., et al.: New opportunities for electricity generation in shallow hot dry rock fields: A study of thermoelectric generators with different heat exchangers. *Energy Conversion and Management*, **200**, (2019), 112061.

Gholamian, E., Habibollahzade, A., Zare, V.: Development and multi-objective optimization of geothermal-based organic Rankine cycle integrated with thermoelectric generator and proton exchange membrane electrolyzer for power and hydrogen production, *Energy Conversion and Management*, **174** (2018.): 112-125.

Lorenz, R.D., Clarke, E.S.: Influence of the Multi-Mission Radioisotope Thermoelectric Generator (MMRTG) on the local atmospheric environment, *Planetary and Space Science*, **193**, (2020), 105075.

Li, K.W., Bian, H.Y., Liu, C.W.: Comparison of geothermal with solar and wind power generation systems, *Renewable and Sustainable Energy Reviews*, **42**, (2015), 1464–1474.

Li, K., Liu, C., Jiang, S., et al.: Review on Hybrid Geothermal and Solar Power Systems, *Journal of Cleaner Production*, **250**, (2019), 119481.

Li, K., Garrison, G., Zhu,Y., et al.: Thermoelectric power generator: Field test at Bottle Rock geothermal power plant. *Journal of Power Sources*, **485**, (2020), 229266.

Qiu, K., Hayden, A.C.S.: Integrated thermoelectric and organic Rankine cycles for micro-CHP system, *Applied Energy*, **97**, (2012), 667–672.

Tohidi, F., Holagh, S.G., Chitsaz A.: Thermoelectric generators: a comprehensive review of characteristics and applications, *Applied Thermal Engineering*, **201**, (2022), 117793.

Xie, H.P., Ang, R., Li, B.X.: principle and technological conception of middle-low temperature geothermal power generation based on large-scale single crystals of thermovoltaic materials, *Advanced Engineering Sciences*, **50**, (2018), 2096-3246.

Xu, Z.Y., Wang, R.Z., Yang, C.: Perspectives for low-temperature waste heat recovery, Energy, **176**, (2019), 1037-1043.

Yang, W., Xie, H.P., Sun, L.C., et al.: An experimental investigation on the performance of TEGs with a compact heat exchanger design towards low-grade thermal energy recovery, *Applied Thermal. Engineering*, **194** (2021), 117119.

Zare, V., Palideh, V.: Employing thermoelectric generator for power generation enhancement in a Kalina cycle driven by low-grade geothermal energy. *Applied Thermal Engineering*, **130**, (2018), 418–428.

Zwab, C., Shuai, Z., Zlab, C., et al.: Thermoelectric converter: Strategies from materials to device application, *Nano Energy*, **91**, (2022), 106692.